Effects of landscape patterns on the summer microclimate and human comfort in urban squares in China

Authors:

1. SHUANG LIU, Lingnan Normal University, school of Life Science and Technology, China, liushuangaaa@163.com

2. DR. JING ZHAO, corresponding author, University of Lincoln, school of Architecture and the Built Environment, Brayford Pool, Lincoln, U.K., LN6 7TS, jingzhao@Lincoln.ac.uk, +44 7741010213.

3. MINGFENG XU, Guangdong Academy of Forestry, China, 735871702@qq.com

4. EHSAN AHMADIAN, University of Lincoln, school of Architecture and the Built Environment, U.K. eAhmadian@lincoln.ac.uk

ABSTRCT： This research uses empirical data and supplementary computer simulation result to study the summertime cooling effect of different landscape patterns in urban areas in China. It employs field monitoring to collect hourly air temperatures and relative humidity at pedestrian level over five consecutive days in July 2016, and calculates the discomfort index for each scenario in studied urban squares. It also builds simulation models using Citysim and Meteonorm software to further explore the cooling effects of different landscape patterns within the same square. The results from field research show that the difference in cooling and humidification among the four landscape patterns is significant, as is the thermal comfort or discomfort caused by such effect. The research finds that the urban square equipped with

only hard paving and no canopy coverage could cause extreme discomfort and heatstroke during summertime in the studied climate, whereas the urban square with lawn grass, high canopy closure and thick canopy can reduce discomfort. The simulation analysis further confirm that lawn grass can noticeably reduce the ground surface temperature and the surface temperature of the surrounding buildings than if using asphalt as the ground cover. The findings from this research provide design guidance for the landscape configuration of urban squares in similar climates.

Acknowledgements

This work was supported by the Natural Science Foundation of Guangdong Province, China(2018A030307059) and Overseas Scholarship Program for Elite Young and Middle-aged Teachers of Lingnan Normal University

1. Introduction

With the acceleration of urbanisation around the globe, the urban heat island (UHI) effect, is the most prominent climate characteristic and an important factor affecting the liveability of urban environments (Grimmond et al., 2010; Oke, 1978). Under the influence of the UHI effect, extreme high temperature weather patterns occur frequently in summer, causing human discomfort and in extreme cases, casualties. For example, during the summer of 2003, western Europe experienced one of the worst heat waves in recent history, with an estimated excess mortality varying between 25,000 and 70,000 (D'Ippoliti et al., 2010). From 2000 to 2016, the annual estimated number of people worldwide affected by a heat wave was

125 million (Watts et al., 2018), causing the use of energy-intensive cooling devices such as air-conditioning, leading in turn to higher energy consumption and pollutant emissions (Fouillet et al.,2006; Wu et al., 2013). Meanwhile, the UHI effect has created localised circulation within the urban area where the retention of heat and pollutants in the city centre has been exacerbated, resulting in an escalating deterioration of the urban environment (Fouillet et al., 2006).

Research suggests that the UHI effect can be mitigated at a microscale by modifying the urban microclimate (Bernatzky, 1982; Ca et al.,1998; Kawahsima, 1990). Vegetation cover is the main climate modifier in urban areas (Oke, 1989; Vieira de Abreu-Harbich et al., 2015; Salmond et al., 2016; Li et al., 2016; Mushtaha et al., 2021). Green landscapes such as parks, squares and green areas can modify the microclimate by reducing temperature and increasing humidification, thus alleviating the UHI effect (Rahman et al., 2011; Oliveira et al., 2011; Konarska et al., 2014; Norton et al., 2015). In particular, urban canopy structures can modify local microclimate by shading direct shortwave radiation, thereby altering the surface energy balance and reducing surface temperatures (Rahman et al., 2011; Lindberg and Grimmond 2011). Transpiration in urban green areas can effectively reduce the air temperature, increase the relative humidity, and improve the microclimate of the surrounding environment (Jauregui, 1990-1991; Avissar, 1996; Madureira et al., 2015; Xue, et al., 2016).

The design of greenery in urban squares varies greatly in order to meet different functions, but up to now the design has mostly been guided by aesthetic preferences (Erell,

2008). In recent years, however, increasing attention has been paid to the microclimatic benefits of urban green areas in terms of form and distribution (Xue et al., 2017; Sodoudi et al., 2018; Zhao et al., 2018). Previous studies that focused on small-scale urban landscape have been informative for understanding context-based microclimate and providing design guidance in the use of green landscapes to modify urban microclimate. Research has shown that many factors can influence the effectiveness of vegetation for cooling and humidification (Rahman et al., 2020； Gao et al., 2018; Brown et al., 1995; Wu et al., 2016). The dominant factors include the area of vegetation (Jiao et al., 2017), vegetation type (Du et al., 2018; Wu et al., 2016) and the configuration of vegetation cover (Zölch et al., 2019). Research by Armson et al. (2012) examined the role of trees and grasses in reducing temperatures in an urban area. They chose a small plot in the UK and reported that while both grass and trees effectively reduced the surface temperature and served to mitigate UHI in hot weather, tree shade more effectively reduced local air temperature. Similarly, Rahman et al. (2018) examined the below-canopy vertical air temperature gradients of urban trees and suggested that, when the days are very hot, canopy cooling is more beneficial in comparison with grass surface evapotranspirational cooling. More small-scale urban landscape research is urgently needed, especially in subtropical and tropical regions with very hot summertime temperatures, in order to inform stakeholders and urban designers and improve the urban microclimate.

This research employed field monitoring data and a supplementary computer simulation model to study the effect of landscape patterns on the outdoor thermal environment in

Zhanjiang, China. Zhanjiang experiences both tropical and subtropical monsoon climates with hot, humid summers and mild winters. The research took four different landscape patterns in urban squares in Zhanjiang as case studies; investigated and compared the cooling and humidification effects on the microclimate during summertime using monitored temperature and humidity data. The characteristics of the landscape patterns taken into consideration included different underlying substrates, tree species, crown width, canopy coverage and canopy closure. The research further explored the specific effect of ground cover with a computer simulation modelled on one of the case studies, using a 10-year average of meteorological data in order to gain further insight into the underlying effect of landscape patterns on ground surface temperature and the surface temperature of surrounding buildings over a longer time period.

2. Research Methods

2.1 Overview of the research sites

Zhanjiang City is located on Leizhou Peninsula, the southernmost part of mainland China, between 109°31′—110°55′ E and 20°12′—21°35′ N. The average annual temperature in Zhanjiang is approximately 23°C, with an average humidity of 81% and dew point at 20°C (Luo et al., 2017). The prevailing wind direction is from the south, with an average annual wind speed between 1 and 3m/s. The average annual sunshine hours is between 1817 and 2106h, and the average annual rainfall is between 1417 and 1802mm (Luo et al., 2017). The hottest period usually occurs during July and August, with maximum temperatures reaching

38°C. Zhanjiang has a small temperature difference between day and night in summer, where the average wind speed in July is 2m/s.

Lingnan Normal University is located in the urban area of Zhanjiang and covers an area of approximately 67 hectares. Four squares within the university campus were chosen as case studies. The squares had distinctive landscape patterns, yet were typical of the climate in an urban context. Square A was rectangular with an area of approximately 4,500m^2, had buildings on two sides and an outdoor stage on another. It was paved with concrete, with no trees or shrubs. Due to the absence of vegetation, this square was selected as a control point. Square B was nearly elliptical, with an area of approximately 13,000m^2, it had buildings on both sides. It was covered by lawn grass (*Zoysia tenuifolia*), but without trees or shrubs. Square C was rectangular with an area of approximately 4,850m^2 and had buildings on two sides. It was covered by lawn grass (*Zoysia tenuifolia*), and sparsely planted coconut trees (*Cocos nucifera*). Square D was rectangular with an area of approximately 3,650m^2, surrounded by buildings on three sides. It was paved with concrete and planted with dense Chinese Banyan tress (*Ficus microcarpa*). Apart from square B, the areas of the studied squares were similar. The occupancy of each square was varied and mobile throughout the day. The detailed landscape patterns of each square are shown in Table 1, images of the squares are shown in Figure 1.

Table 1 Landscape pattern characteristics of four studied cases

ID	Different square landscape patterns	The average DBH/cm[1]	Average tree height/m	Average crown diameter/m	Canopy density[2]	Groundcover plant
A	Hard paving	-	-	-	-	no
B	Lawn grass（*Zoysia tenuifolia*）	-	-	-	-	*Zoysia tenuifolia*
C	Coconut tree (*Cocos nucifera*) + Lawn grass (*zoysia tenuifolia*）	23.48 ± 4.41	11.14 ± 2.57	5.56 ± 2.65	0.48 ± 0.16	*Zoysia tenuifolia*
D	Chinese banyan tree (*Ficus microcarpa*)+hard paving	38.36 ± 6.26	16.26 ± 3.52	10.24 ± 3.21	0.95 ± 0.03	no

Square A

Square B

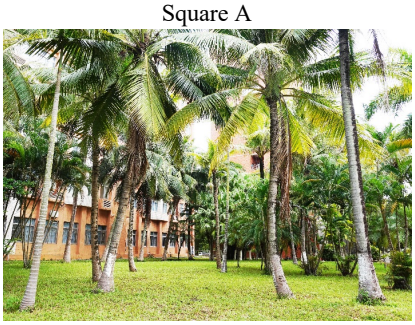

Square C

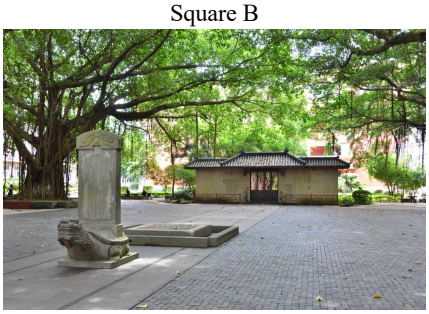

Square D

Figure 1 Images of four studied cases

2.2 Microclimate measurements

The microclimate measurements were taken using HOBO U23-001 temperature and humidity recorder, with capacity for continuous measurement outdoors. The recorder had a temperature range of -40°C to 70°C and a relative humidity range of 0–100% RH (Temperature test accuracy ± 0.21°C, relative humidity test accuracy ± 2.5%). The

[1] DBH: Diameter at breast height
[2] Canopy density was measured with hemispherical photography

measurements were conducted in all four squares simultaneously for five sunny and windless days (wind speed of ≤ 2 m/s) in July 2016. The Data was collected at hourly intervals from 8:00 to 18:00. Each square had five measurement points from which data was taken to find an average. For rectangular squares, the measurement points were located at 1/4 and 3/4 of the diagonals of the square, and at the intersection of the diagonals. For the elliptical square (square B), first the ellipse was divided into four even quadrants, then the middle of each arc joined into a rectangular shape; the measuring point was subsequently set according to the rectangular square method. It should be noted that as there was a path in the middle of the oval square, this central measurement point was adjusted to a point 10m to the left along the diagonal intersection to avoid the effect of the path on the measured data (Figure 2). The four sites were all semi-open, surrounded by buildings on two or three sides. In order to minimize the interference of surrounding buildings on the result, measurement points were chosen further away from the borders or four corners of the sites. The HOBO was installed 1.5m from the ground to measure the air temperature and humidity at pedestrian level.

Figure 2 Diagram of selected measurement points.

2.3 Discomfort index

Human health is greatly affected by weather and climatic factors such as temperature (Basu, 2009) and humidity (Qu and Xiao, 2019). This research chose to use the Discomfort Index (DI) to quantify comfort/discomfort levels experienced by the human body. The DI was previously proposed by Thom (1959) as it had been widely adopted in a similar field due to its simple parameters, less restrictive test conditions, and more convenient correlation analysis. It is especially suitable for the evaluation of human body thermal comfort in an outdoor environment (Georgi et al., 2006; Wu et al.,2019). The DI was calculated using two indicators that affect the human body, namely temperature and humidity. The calculation formula is as follows:

$$DI = t - 0.55 \times (1 - 0.01 \times RH) \times (t - 14.5)$$

In the formula: DI indicates the discomfort index; t is the air temperature; RH is the relative humidity of the air. The DI reflected the degree to which the human body felt comfortable with the air environment under certain conditions of temperature and humidity. Table 2 shows the classification criteria for the DI.

Table 2 Discomfort index evaluation (Yan et al. 2012; N. J. Georgi et al., 2006)

Grade	Discomfort Index	Feeling Degree
1	< 21.0	No one is uncomfortable
2	21.0 - 23.9	A small number of people feel uncomfortable
3	24.0 - 26.9	many people feel uncomfortable
4	27.0 - 28.9	Most people feel uncomfortable
5	29.0 - 31.9	Almost everyone feels uncomfortable
6	> 32.0	Risk of heatstroke

2.4 Calculation and Data Processing Methods

Indicators such as temperature difference and drop rate were calculated using the formula below:

$$\text{Cooling rate} = \frac{t_{sun} - t_{sh}}{t_{sun}} \times 100\%.$$

In the formula, t_{sun} is the average temperature of the control point (square A), and t_{sh} is the average temperature of each studied square. The calculation for humidification rate and discomfort reduction rate used a similar formula.

Field measurement data was processed by STATISTICA10.0. STATISTICA is a professional mathematical statistics software developed by StatSoft in the United States, widely used for statistical analysis for its graphical data representation capabilities. In STATISTICA 10.0, statistical descriptions and one-way analysis of variance were performed on indicators such as temperature, relative humidity, cooling and humidification, and reduction of DI. The differences between the groups were analysed by LSD multiple comparison. The charts were all performed in STATISTICA 10.0. Data sorting, screening, sorting, etc. were performed in Excel 13.0.

2.5 Using Meteonorm and CitySim

The second stage of the research utilised simulation software to model the environment of square B in order to simulate different scenarios with consistent peripheral parameters. The energy simulation software, CitySim, was selected due to its urban simulation function that considers influential parameters used for urban analysis such as surface temperature, radiative inter-reflection between surfaces and shadowing effect

(Ahmadian et al., 2019), as well as its superior representation of surface and building characteristics, and advanced capabilities for radiation exchange calculations from a set of urban buildings (Sola et al., 2020). CitySim had been adopted for several previous studies investigating urban energy analysis. Le Guen et al. (2018) used CitySim for improving energy sustainability of a village in Switzerland through integration of building renovation and renewable energy. Perera et al. (2018) combined CitySim with an urban climate model and an energy system optimization model to show the impact of urban climate on urban energy demand. Moghadam et al. (2019) adopted CitySim to develop a new visualization method for the evaluation of urban heat energy planning scenarios. CitySim has been previously validated using both monitored data and other energy simulation software. Specifically, Ahmadian et al., (2021) validated CitySim through a pilot investigation, comparing the results with a previously reported SAP (Standard Assessment Procedure) prediction model. Also, Coccolo et al. (2013) validated CitySim against EnergyPlus software using two existing buildings. Furthermore, Walter and Kämpf (2015) validated CitySim against BESTEST for calculating annual and peak heating/cooling energy demand of buildings. They also experimentally verified the tool using monitored data of the annual heating consumption of an EPFL campus building.

In this research, square B was chosen as the base simulation model because of its lack of canopy coverage and defined enclosure created by surrounding buildings. This allowed CitySim to create a more enclosed system to compare different scenarios, specifically in order to study the effect of ground cover. By using Meteonorm (Remund et al., 2015) to obtain a 10-year average temperature and solar radiation data in the studied urban area, the

simulation provided an accurate long-term result when comparing the modelled scenarios. The simulation focused specifically on the ground cover landscape patterns and their effect on the microclimate. The simulation monitored the surface temperature of the ground (square B) and the surface temperature of surrounding buildings that enclosed square B over a 10-year period from 2010-2019 under two scenarios. The first simulated scenario followed the actual condition of the square, with lawn grass as the main landscape pattern. The second scenario substituted the lawn grass for asphalt. For each scenario, the parameters are defined in Table 3 as follows (Upadhyay et.al, 2015):

Table 3 Simulation parameters defined for grass and asphalt scenarios

Scenarios	Composition	Thickness m	Density kg/m³	Cp (Specific Heat Capacity) J/(kg K)	Conductivity W/(m K)	Shortwave Reflection	kFactor
S1 - Lawn Grass	**Clay**	0.025	1760	920	0.97	0.21	0.7
	Loam	0.05	1800	864	1.4		
	Sand	0.05	1300	828	0.5		
	Molasse	0.875	1600	1200	2.4		
S2 - Asphalt	**Cast asphalt**	0.025	2360	1200	0.75	0.14	0
	Sand	0.05	1300	828	0.5		
	Gravel	0.05	1800	792	0.7		
	Molasse	0.875	1600	1200	2.4		

The surrounding building parameters were obtained from the Estate department in Lingnan Normal University and were applied in both scenarios (Table 4):

Table 4 Simulation parameters defined for surrounding buildings

	Walls of Surrounding buildings	**Roofs of Surrounding buildings**
Construction	Masonry cavity wall	Masonry Reinforced concrete
U-Value W/m²K	1.4 /1.3 (glazing)	0.85
G-Value	0.55	n/a
Short-wave reflectance	0.6	0.2
Conductivity	Composite (See appendix)	Composite (See appendix)

The selected sets of simulation results for comparison included the surface temperature of the simulated square (ST_g) and the surface temperature of the external façade of surrounding

buildings facing the square (ST_w_SW for the row of façade facing Southwest and ST_w_NE for the row of façade facing Northeast). The statistical analysis used SPSS software. The simulation model included the central square as well as the surrounding buildings (Figures 3a and 3b).

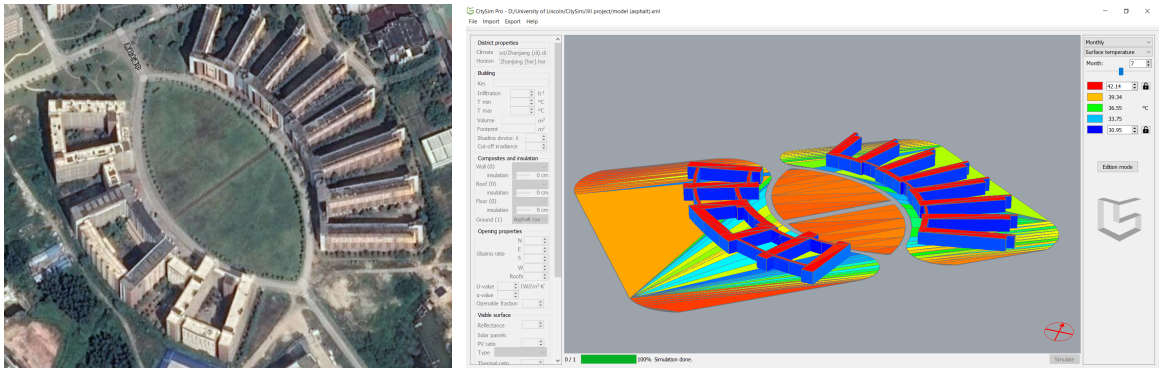

Figure 3a Aerial view of square B; Figure 3b simulation process model using CitySim

3. Results from monitored data

3.1 Cooling and humidification effect of different landscape patterns

As shown in Figure 4, the temperature during any given daily period showed significant differences in all measured squares. The temperature in square A was significantly higher than that in the other squares from 9:00 to 18:00. The temperature in square B was very close to that in square C. The temperature in square D was lower than that in all the other squares during the whole period, indicating a greater cooling effect in square D. The daily cooling rate of each square showed a similar trend to the daily temperature fluctuations of corresponding squares.

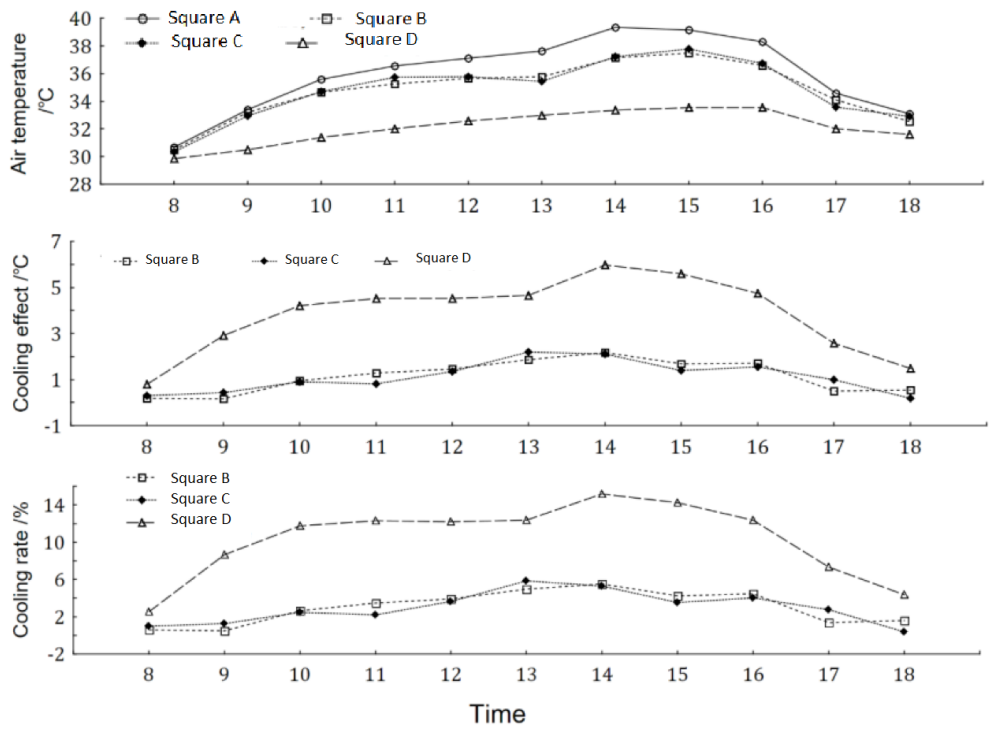

Figure 4 Comparison of diurnal changes of air temperature indexes in different squares

The cooling effect of the various landscape patterns were calculated using square A as the control point. The analysis of multiple comparison results of temperature (Table 5) showed that square D exhibited the best cooling effect compared with square B and square C ($P < 0.05$). The difference in cooling rate between squares B and C was very small. Moreover, squares A, B and C all had higher temperature fluctuations throughout the day, whereas the hourly temperature was more consistent in square D.

Table 5 Difference of landscape cooling effect in different squares

	air temperature/℃				Temperature difference/℃				Cooling rate /%			
ID	average value	Minimum value	Maximum	Coefficient of variation /%	average value	Minimum value	Maximum	Coefficient of variation/ %	average value	Minimum value	Maximum	Coefficient of variation/ %
A	35.94a	29.87	40.54	8.12	0.00 a	0.00	0.00	0.00	0.00 a	0.00	0.00	0.00
B	34.80 b	29.55	38.30	6.57	1.14 b	-0.85	3.23	81.58	3.03 b	-2.56	7.97	80.98

C	34.83 b	30.11	38.13	6.47	1.11 b	-1.53	3.50	94.98	2.94 b	-4.99	8.63	95.39
D	32.13 c	29.40	36.65	4.73	3.82 c	0.15	8.85	49.53	10.30 c	0.48	21.98	45.16

Note: the lowercase letter after the average value is a multiple comparative analysis of the cooling effect between different squares (LSD difference test, different letters indicate significant differences, $P < 0.05$).

The calculation of humidification rate employed the same method as the calculation for cooling rate, using sqaure A as the control point. The hourly humidity and humidification rate of the four studied sites also showed significant differences. The relative daily humidity showed a single wave valley pattern. The lowest humidity was recorded at 14:00 in square A, 15:00 for squares B and C, and 16:00 for square D. This pattern was consistent with the daily temperature changes in the corresponding squares, indicating that the air temperature was closely correlated with relative humidity. The relative humidity of square A was significantly lower than other squares during the day. Square D had the highest relative humidity at all times of the day. The result of the humidification rate comparison among the four squares was similar to the cooling rate comparison. Square D had the highest humidification rate compared with squares B and C, though no significant difference between squares B and C ($P < 0.05$) was observed.

3.2 Differences in discomfort index between the different squares

Based on the measured temperature and humidity results, the hourly DI was calculated (Table 6). According to the hourly DI of the different squares, square A had the highest average and maximum value, whereas square D had the lowest, indicating that square D provided more comfort in terms of temperature and humidification. The discomfort rate of

squares B and C were similar. The DI also showed that the highest level of discomfort appeared in square A at 14:00 and 15:00, indicating the risk of heatstroke. Square D had the lowest DI at 8:00, 9:00, 17:00, and 18:00 with level 4 discomfort.

Table 6 Evaluation of discomfort Index in different squares

time	Square A	level	Square B	level	Square C	level	Square D	level
8:00	28.91	4	28.77	4	28.66	4	28.35	4
9:00	30.05	5	30.18	5	29.89	5	28.61	4
10:00	31.06	5	30.87	5	30.57	5	29.00	5
11:00	31.24	5	31.01	5	30.93	5	29.26	5
12:00	31.44	5	31.11	5	30.90	5	29.51	5
13:00	31.71	5	31.22	5	30.95	5	29.74	5
14:00	32.21	6	31.67	5	31.55	5	29.80	5
15:00	32.27	6	31.94	5	31.67	5	29.91	5
16:00	31.83	5	31.30	5	31.11	5	29.78	5
17:00	29.95	5	29.98	5	29.58	5	28.70	4
18:00	29.34	5	29.18	5	29.24	5	28.49	4
Average	30.91		30.66		30.45		29.19	
Maximum	32.27		31.94		31.67		29.91	
Minimum	29.34		29.18		29.24		28.49	

For the majority of the measured time periods the DI in all squares was at level 5, which meant that almost everyone felt uncomfortable. Such a result was not unusual in the studied climate region. In general, it is not advised to stay outside for an extended period of time. However, the result suggests that with certain configurations of landscape design, the discomfort can be reduced effectively.

4. Simulation of square B

The second stage of this research employed a computer simulation method using CitySim with climate data provided by Meteonorm. The reasons for performing the simulation were: (1) By using 10-year average climate data collected by Meteonorm in digital simulation, a long-term effect of different ground covers could be explored to supplement the measured result. (2) The simulation enabled comparison of different ground covers in a controlled

environment where all other conditions could be kept unchanged. (3) Combining the 3D model and climatic data with CitySim simulations could potentially provide new ideas and additional decision-making tools for urban planning and microclimate simulation research in different regions.

The simulation used the 10-year average meteorological data to provide a long-term microclimatic result for two scenarios: the first followed the actual condition of the square, with lawn grass as the main landscape pattern; the second scenario exchanged the lawn grass with asphalt to explore the difference this made to the microclimate. The surface temperature on the central ground for the two simulated scenarios are shown in Figure 5. The temperatures for both scenarios show a similar trend throughout the day, with the maximum temperature recorded at 14:00. The surface temperature of asphalt was consistently higher than that of grass. The highest mean temperature of asphalt ground was 53^{o}C, the highest temperature of grass ground was 32^{o}C. The mean temperature difference was 5.7^{o}C throughout the 10-year simulated period with a paired sample t-value of 74.64 ($p < 0.001$), where the highest hourly mean temperature difference was nearly 19^{o}C occurring at 13:00 and 14:00.

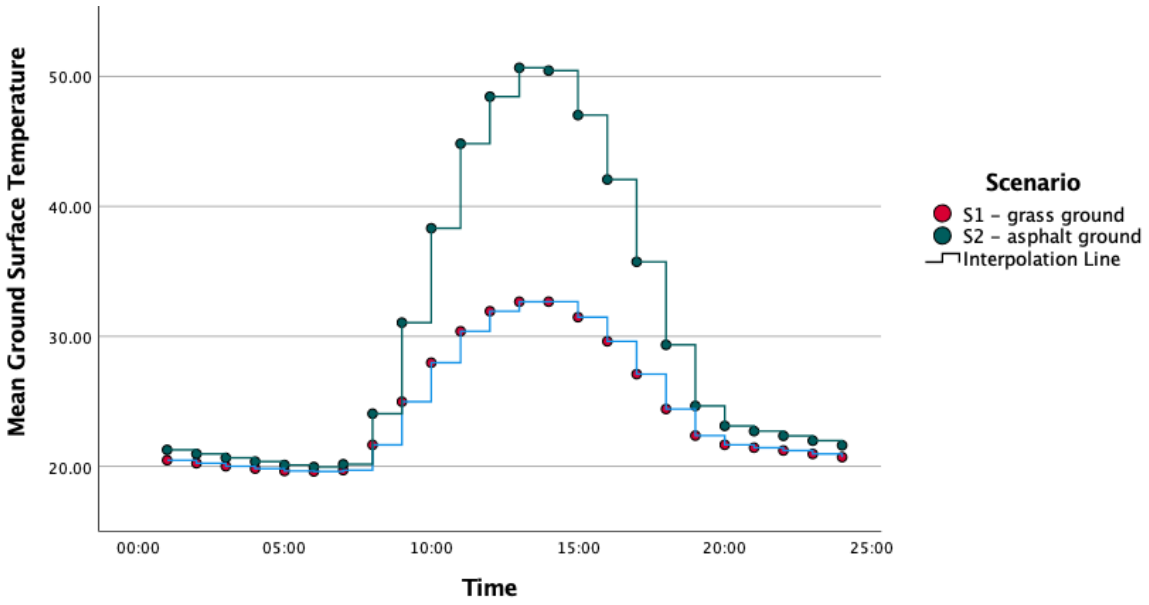

Figure 5 Comparison of ground surface temperature (ST_g) between two scenarios

The simulation result can be further compared based on the monthly average ground surface temperature (Figure 6) over the 10-year time period between 2010-2019. The result showed a significant difference in surface temperature between the two scenarios. This difference was more apparent during summertime (July and August), where the mean monthly temperature difference could reach 10°C between grass ground and asphalt ground.

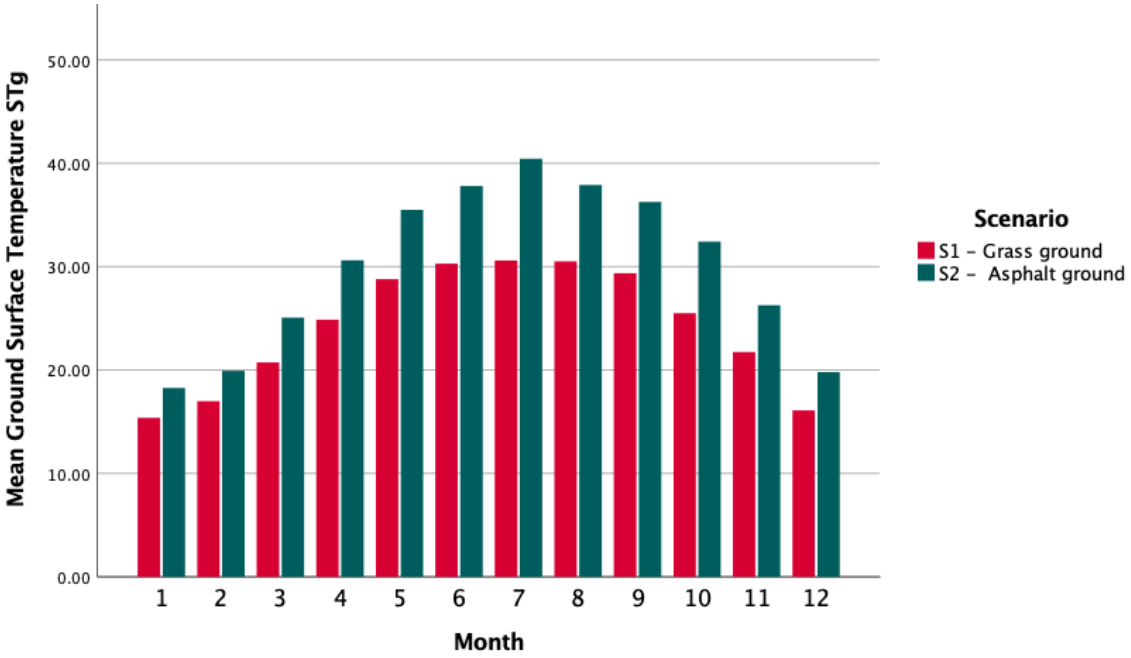

Figure 6 Mean ground surface temperature (ST_g) by month by scenario (2010-2019 average)

Additionally, a more interesting comparison was found when comparing the surface temperature of the surrounding buildings between the two scenarios (Figure 7). The façades facing the square were separated into two groups based on their orientation, Southwest (SW) and Northeast (NE), and the temperatures of each group in both grass and asphalt scenarios were compared. The group of façades facing SW had a higher mean temperature throughout the day and throughout the year, which was to be expected at the given geographic location in the Northern hemisphere. The façades facing both directions showed a similar mean temperature difference of 0.5°C between two simulated scenarios with a paired sample t-value of 104 and 106 respectively ($p < 0.001$). The maximum temperature difference for the SW facing façades was 2.63°C while for the NE facing façades, the maximum temperature difference was 2.81°C.

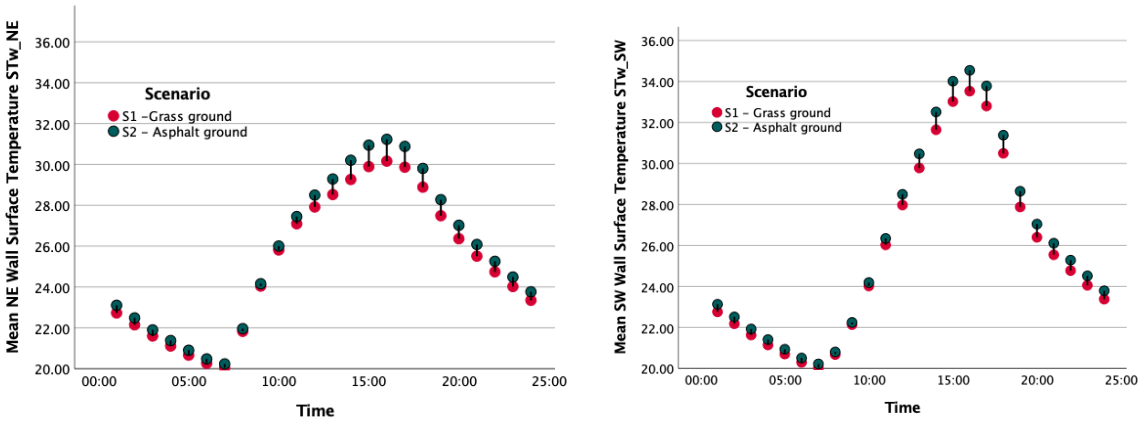

Figure 7 Comparison of NE and SW external wall surface temperature (ST_w) between two scenarios

5. Discussion

According to the data analysis of monitored temperature and humidity, when comparing the cooling effect between squares C and D, it is interesting to note that despite square C employing both canopy cooling and grass evapotranspirational cooling, compared to square D with only green canopy structure as the cooling mechanism, the advantage of square D in cooling and humidification is apparent. The significant advantage exhibited in square D from the monitored result confirmed that wider tree crowns and higher density canopy provided a better cooling effect, as had been reported by Speak et al., (2020). This is also consistent with the research findings provided by Li et al. (2011) that tall trees forming an arbour can achieve a better cooling effect than shrubs and lawns with the same footprints. The result also suggested that canopy vegetation with a larger crown size and coverage is more effective in reducing local air temperature than grass surface evapotranspirational cooling in very hot weather. This result was similar to the result reported by Armson et al. (2012) and Rahman et al. (2018). The comparison of the humidification effect showed that on a hot summer day, the humidification effect of green space is particularly significant, in comparison with outdoor areas covered with no shade and only hard paving . This result is consistent with research conducted by Wu et al. (2013). The humidification result confirmed that plant transpiration

can effectively increase the cooling effect (Tanaka and Hashimoto, 2006; Dixie and Johnson, 2004). Plant transpiration produces large amounts of water vapour, which increases the local air vapour content and thus the relative humidity. Higher crown and denser canopy can increase the total area of plant leaves and the corresponding high transpiration of water vapour (Qin et al., 2015; Foley et al., 2003).

When comparing squares B and C, it is interesting to note that even though square C had large areas of green canopy coverage, whereas square B had none, the cooling and humidification effects were very similar. The reason that no significant difference in cooling and humidification effect was found between the two squares in this research might be because the area of square B was much larger than that of square C, resulting in a larger green area hence a higher rate of humidification (Jiao et al., 2017; Gioia et al., 2014; Chang et al., 2007).

The DI result confirmed that the outdoor summertime comfort level for humans is higher in an area with green vegetation than in an area with only hard paving and no greenery. This result is consistent with a number of previous studies (Wu et al., 2020; Akbari, 2002; Mayer et al., 2008; Streiling et al., 2003); it also suggested that higher tree coverage with large canopy closure and a thick canopy can significantly reduce the DI and the risk of heatstroke, which is consistent with the research conducted by Rahman et al. (2020) and Georgi et al. (2006). This result also confirms the findings reported by Feng et al. (2014) that urban squares dominated by arboreal structures provide better comfort, and the comfort level increases with the increase of canopy closure.

The simulation of square B suggested that lawn grass can effectively reduce the ground surface temperature, in comparison with asphalt ground. The annual average difference in

ground surface temperature was 5.7°C. This result is reflected in previous research which suggests that different heat capacity, thermal conductivity, warming rates and albedo of different ground surfaces, can significantly affect the surface temperature of the ground (Wu et. al., 2013; Shang et. al., 2019). The latent heat consumed by the lawn due to plant transpiration and evaporation was greater than asphalt, which greatly reduced the heat storage of green space and the heat exchange between ground and air, hence the grass covered ground gained less heat, resulting in a reduced surface temperature. This result is consistent with previous research by Coccolo et al. (2018) that greening and cooling materials could effectively reduce surface temperatures. The comparison of mean monthly temperature result is consistent with previous research conducted by Upadhyay et. al (2015), confirming that grass covered ground has a better cooling effect than concrete or asphalt covered ground. Moreover, the simulation also suggested that using lawn grass as a landscape material could also reduce the surface temperature of the surrounding buildings, due to a reduction in net ground radiation. The mean reduction, however small, was significant in the paired sample t-Test. This result is consistent with research conducted by Mansouri (2017) that the albedo effect of the ground cover could impact the air and surface temperature of surrounding buildings.

6. Conclusion

This research employed field monitoring data and supplementary computer simulation results to study the effect of landscape patterns on the outdoor thermal environment in Zhanjiang, China. The primary findings of this research confirm that urban landscape

configurations can effectively alter the outdoor thermal environment on a micro-scale to mitigate the UHI effect. Especially in tropical and subtropical climatic regions, canopy vegetation with a large crown size and coverage can significantly reduce summertime discomfort and the risk of heat stroke in built-up urban areas. Further simulation results, which specifically studied ground cover landscapes, found that green vegetation, in comparison with hard paving covered ground such as asphalt, can not only reduce the surface temperature of the ground area consistently over a longer time period, but also has a detectable cooling effect on the façades of surrounding buildings.

7. Limitation and future research

It is important to acknowledge that the existence of a number of limitations during the research design process may have affected the findings. Firstly, the field measurement was conducted during a 5-day period in 2016. A lack of longer-term and repeated observation could limit the validity and generalisability of the result. Furthermore, due to limitations of resources, certain meteorological variables (such as wind speed) were not measured. Although previous research without the consideration of wind speed showed conclusive results (Talukdar et al., 2018; Zheng et al., 2020), future research should take such measures into consideration, even if the effect is minimal. It would also be beneficial to consider alternative comfort indexes that take wind speed into consideration to measure comfort levels in future research. Secondly, due to a lack of resources, no occupancy or qualitative data was collected during the monitored time period to compare with the measured data and calculated DI result. Further research is needed to allow for a longer monitored time period

accompanied by a questionnaire survey on the subjective measure of outdoor comfort. Lastly, the simulation only modelled one square with two different scenarios using lawn grass and asphalt as the ground covering. The result from the simulation could be further strengthened with more scenarios modelling different landscape patterns, where the effect of canopy coverage could be added to the simulation. At the same time, the simulation could further benefit from measured data (such as albedo) as input data, in order to draw conclusion on a broader scale.

References

Ahmadian, E., Sodagar, B., Bingham, C., Elnokaly, A. & Mills, G. (2021). Effect of urban built form and density on building energy performance in temperate climates. Energy and Buildings. Volume 236, 2021, 110762, ISSN 0378-7788, https://doi.org/10.1016/j.enbuild.2021.110762.

Ahmadian, E., Sodagar, B., Mills, G., Bingham, C. (2019). Correlation of urban built form, density and energy performance. Journal of Physics: Conference Series https://iopscience.iop.org/issue/1742-6596/1343/1

Akbari, H. (2002). Shade trees reduce building energy use and CO 2 emissions from power plants. Environmental Pollution, Volume 116, Supplement 1, 2002, Pages S119-S126, ISSN 0269-7491, https://doi.org/10.1016/S0269-7491(01)00264-0.

Armson, D., Stringer P., Ennos A.R. (2012). The effect of tree shade and grass on surface and globe temperatures in an urban area. Urban Forestry and Urban Greening, 11, 245-255. http://dx.doi.org/10.1016/j.ufug.2012.05.002

Avissar, R. (1996). Potential effects of vegetation on the urban thermal environment. Atmospheric Environment,1996, 30(3), 437-448. https://doi.org/10.1016/1352-2310(95)00013-5

Basu, R. (2009). High ambient temperature and mortality: a review of epidemiologic studies from 2001 to 2008. Environmental Health, 2009, 8: 40. doi:10.1186/1476-069X-8-40

Bernatzky, A. (1982). The contribution of tress and green spaces to a town climate. Energy and Buildings,5(1),1-10. https://doi.org/10.1016/0378-7788(82)90022-6

Brown, R.D., Gillespie, T.J. (1995). Microclimate Landscape Design: Creating Thermal Comfort and Energy Efficiency. John Wiley & Sons, Chichester.

Ca, V. T., Asaeda, T., Abu, E. M. (1998). Reductions in air conditioning energy caused by a nearby park. Energy & Buildings, 29(1),83-92. info:doi/10.1016/S0378-7788(98)00032-2

Chang, C.R., Li, M.H., &Chang, S.D.(2007). A preliminary study on the local cool-island intensity of Taipei city parks. Landscape Urban Planning. 80, 386–395. http://dx.doi.org/10.1016/j.landurbplan.2006.09.005

Coccolo, S., Kämpf, J.H. & Scartezzini, J.-L. (2013). Design in the desert. A Bioclimatic project with urban energy modelling. Proceedings of BS2013: 13th Conference of International Building Performance Simulation Association, Chambéry, France, August 26-28

Coccolo, S., Kämpf, J., Mauree, D., Scartezzini, J.-L. (2018) Cooling potential of greening in the urban environment, a step further towards practice. Sustainable Cities and Society, Volume 38, Pages 543-559, ISSN 2210-6707,https://doi.org/10.1016/j.scs.2018.01.019.

D'Ippoliti D., Michelozzi P., Marino C., de'Donato F., Menne B., Katsouyanni K., Kirchmayer U., Analitis A., Medina-Ramón M., Paldy A., Atkinson R., Kovats S., Bisanti L., Schneider A., Lefranc A., Iñiguez C., Perucci CA. (2010). The impact of heat waves on mortality in 9 European cities: results from the EuroHEAT project. Environ Health. 2010 Jul 16;9:37. doi: 10.1186/1476-069X-9-37.

Dixie, L., Johnson, L. (2004). Vegetation-mediated changes in microclimate reduce soil respiration as woodlands expand into grasslands. Ecology, 85(12), 3348-3361. https://www-jstor-org.proxy.library.lincoln.ac.uk/stable/3450514

Du, W., Wang, C., Wang, Q. Bao, H., He, R., Xu, C., Gao, F., Xie, J. (2018). Evaluation of Summer Environmental Effects of the Main Vegetation Types in Beijing Fragrant Hills Park. Scientia Silvae Sinicae, 54, 155-164. DOI: 10.11707/j.1001-7488.20180418

Erell, E., (2008). cThe application of urban climate research in the design of cities, Adv. Build. Energy Res, 2 (1) 95–121. https://doi.org/10.3763/aber.2008.0204

Feng Y., Li E., Zhang L. (2014). Microclimate Effects of Campus Green Space in Summer. Acta Scientiarum Naturalium Universitatis Pekinensis, 50 (5):812-818.DOI: 10.13209/j.0479-8023.2014.085

Foley, J. A., Costa, M. H., Delire, C., Ramankutty, N., Snyder P. (2003). Green surprise? How terrestrial ecosystems could affect earth's climate. Frontiers in Ecology and the Environment, 1(1): 38-44. https://www-jstor-org.proxy.library.lincoln.ac.uk/stable/3867963

Fouillet A., Rey G., Laurent F., Pavillon G.,Bellec S., Guihenneuc-Jouyaux C., Clavel J., Jougla E., Hemon D. (2006). Excess mortality related to the August 2003 heat wave in France. Int Arch Occup Environ Health,80,16–24. DOI: 10.1007/s00420-006-0089-4

Gao Y., Rong L., Li S. (2018). Comparative Effects of Two External Environment Types on the Temperature and Humidity of Urban Green Behs. Journal of Northwest Forestry University, 33(1), 262-268. DOI: 10.3969/j.issn.1001-7461.2018.01.43

Georgi, N.J., Zafiriadis, K. (2006). The impact of park trees on microclimate in urban areas. Urban Ecosystems, 9(3), 195-209. http://explore.bl.uk/primo_library/libweb/action/display.do?tabs=detailsTab&gathStatTab=true&ct=display&fn=search&doc=ETOCRN193100100&indx=1&recIds=ETOCRN193100100

Gioia, A., Paolini, L., Malizia, A., Oltra-Carrio, R., Sobrino, J. A.(2014). Size matters: vegetation patch size and surface temperature relationship in foothills cities of northwestern Argentina. Urban Ecosyst. 17, 1161–1174. http://dx.doi.org/10.1007/ s11252-014-0372-1

Grimmond, C.S.B., Blackett, M., Best, M. J., Barlow, J., Baik, J.-J., Belcher, S. E., Bohnenstengel, S. I., Calmet, I., Chen, F., Dandou, A., Fortuniak, K., Gouvea, M. L., Hamdi, R., Hendry, M., Kawai, T., Kawamoto, Y., Kondo, H., Krayenhoff, E. S., Lee, S.-H., Loridan, T., Martilli, A., Masson, V., Miao, S., Oleson, K., Pigeon, G., Porson, A., Ryu, Y.-H., Salamanca, F., Shashua-Bar, L., Steeneveld, G.-J., Tombrou, M., Voogt, J., Young, D. and Zhang, N. (2010) The International Urban Energy Balance Models Comparison Project: First Results from Phase 1. Journal of Applied Meteorology and Climatology, 49 (6). pp. 1268-1292. ISSN 1558-8432 doi: https://doi.org/10.1175/2010JAMC2354.1 Available at http://centaur.reading.ac.uk/17263/

Jauregui, E. (1990-1991). Influence of a large urban park on temperature and convective precipitation in a tropical city. Energy and Buildings, 15, 457-463 https://doi.org/10.1016/0378-7788(90)90021-A

Jiao, M., Zhou, W., Zheng, Z., Wang, J., Qian, Y. (2017). Patch size of trees affects its cooling effectiveness: A perspective from shading and transpiration processes, Agricultural and Forest Meteorology, 247,293–299. http://dx.doi.org/10.1016/j.agrformet.2017.08.013

Kawahsima, S. (1990). Effect of vegetation on surface temperature in urban and suburban areas in winter. Energy & Buildings, 15(3-4),465-46DOI: https://doi.org/10.1016/0378-7788(90)90022-B

Konarska, J., Lindberg, F., Larsson, A., Thorsson, S., Holmer, B. (2014). Transmissivity of solar radiation through crowns of single urban trees-application for outdoor thermal comfort modelling. Theor. Appl. Climatol. 117, 363-376

Le Guen, M., Mosca, L., Perera, A.T.D., Coccolo, S., Mohajeri, N., Scartezzini, J.-L. (2018). Improving the energy sustainability of a Swiss village through building renovation and renewable energy integration. Energy and Buildings, 158, 906-923

Li, X.X., & Norford, L.K. (2016). Evaluation of cool roof and vegetations in mitigating urban heat island in a tropical city, Singapore. Urban Climate, 16, 59-74

Lindberg F, Grimmond C.S.B. (2011). The influence of vegetation and building morphology on shadow patterns and mean radiant temperatures in urban areas: model development and evaluation. Theor. Appl. Climatol. 105, 311–323. https://doi.org/10.1007/s00704-010-0382-8

Li, Y., Wang, J., Chen, X., Sun, J., Zeng, H. (2011). Effects of green space vegetation canopy pattern on the microclimate in residential quarters of Shenzhen City. Chinese Journal of Applied Ecology. 22(2):343-349. DOI:10.13287/j.1001-9332.2011.0055

Luo S., Chen D., Chen H. Zhou Y. (2017). Analysis and Evaluationon the Tourism Climate Comfort Degree in Zhanjiang City from 1986 to 2016. Journal of Lingnan Normal University,38(6),147-153

Madureira, H., Nunes, F., Oliveira, J., Cormier, L., Madureira, T. (2015). Urban residents' beliefs concerning green space benefits in four cities in France and Portugal. Urban Forestry & Urban Greening, 14(1), 56-64. https://doi.org/10.1016/j.ufug.2014.11.008

Mansouri, O., Belarbi, R., Bourbia, F. (2017). Albedo effect of external surfaces on the energy loads and thermal comfort in buildings. Energy Procedia, 139, 571-577. https://doi-org.proxy.library.lincoln.ac.uk/10.1016/j.egypro.2017.11.255

Mayer, J.D., Salovey, P., Caruso, D.R. (2008). Emotional intelligence: New ability or eclectic mix of traits? American Psychologist, 63, 503-517

Moghadam, S.T., Coccolo, S., Mutani, G., Lombardi, P., Scartezzini, J-L. Mauree, D. (2019). A new clustering and visualization method to evaluate urban heat energy planning scenarios. Cities, 88, 19-36.

Mushtaha, E. Shareefb, S., Alsyoufc, I., Morid, T., Kayede, A., Abdelrahime, M., Albannaye, S. (2021) ‘A Study of the Impact of Major Urban Heat Island Factors in a Hot Climate Courtyard: The Case of the University of Sharjah, UAE’, Sustainable Cities and Society. doi: 10.1016/j.scs.2021.102844

Norton, B.A., Coutts, A.M., Livesley, S.J., Harris, R.J., Hunter, A.M., Williams, N.S.G. (2015). Planning for cooler cities: a framework to priorities green infrastructure to mitigate high temperatures in urban landscapes. Landsc. Urban Plan. 134, 127-138

Oliveira, S., Andrade, H., Vaz, T. (2011). The cooling effect of green spaces as a contribution to the mitigation of urban heat: A case study in Lisbon. Building & Environment, 46, 2186-2194. doi:10.1016/j.buildenv.2011.04.034

Oke, T.R. (1978). Boundary Layer Climates. Methuen & Co Ltd, London.

Oke, T.R. (1989). The micrometeorology of the urban forest. Philosophical Transaction of the Royal Society B 324, 335-349

Perera, A., Coccolo, S., Scartezzini, J.-L., Mauree, D. (2018). Quantifying the impact of urban climate by extending the boundaries of urban energy system modeling. Applied Energy, 222, 847-860

Qin, Z., Li, Z., Cheng, F., Sha, H. (2015). Impact of canopy structural characteristics on inner air temperature and relative humidity of Koelreuteria paniculata community in summer. Chinese Journal of Applied Ecology, 06, 1634-1640. DOI: 10.13287/j.1001-9332.20150331.019

Qu, F., Xiao, Z. (2019). Assessment of the Impact of Climate Change on Human Health. Advances in Meteorological Science and Technology, 04, 34-47. doi:10.3969/j.issn.2095-1973.2019.04.006

Rahman, M.A., Smith, JG, Stringer, P, Ennos, A.R. (2011) Effect of rooting conditions on the growth and cooling ability of Pyrus calleryana. Urban Forestry & Urban Green, 10,185-192 https://doi.org/10.1016/j.ufug.2011.05.003

Rahman M.A., Moserr-ReischL, A., Gold, A., Rötzer, T., Pauleit, S. (2018). Vertical air temperature gradients under the shade of two contrasting urban tree species during different types of summer days. Science of the Total Environment, 633,100-111. https://doi.org/10.1016/j.scitotenv.2018.03.168

Rahman M.A., Hartmann, C., Moser-Reischl, A., Freifrau von Strachwitz, M., Paeth, H., Pretzsch, H., Pauleit, S., Rötzer, T. (2020). Tree cooling effects and human thermal comfort under contrasting species and sites. Agricultural and Forest Meteorology, 287, 107947. https://doi.org/10.1016/j.agrformet.2020.107947

Rahman, M.A., Moser-Reischl, A., Rötzer, T., Pauleit, S. (2019). Comparing the transpirational and shading effects of two contrasting urban tree species. Urban Ecosystems, 22, 683–697. https://doi.org/10.1007/s11252-019-00853-x

Remund J., Müller, S., Kunz, S. (2015). Meteonorm. Global Metereological Database. Version 7.

Salmond, J.A., Tadaki, M., Vardoulakis, S., Arbuthnott, K., Coutts, A., Demuzere, M., Dirks, K. N., Heaviside, C., Lim, S., Macintyre, H., McInnes, R. N., Wheeler, B. W. (2016). Health and climate related ecosystem services provided by street treesin the urban environment. Environmental Health, 15, S36

Shang, R., Li, J., Li, W., Xiao, J., Ren, B. (2019). Different Underlying Surfaces of Urban Green Space in Beijing: Effects on Environmental Microclimate.Chinese Agricultural Science Bulletin, 35(22):77-83. http://www.casb.org.cn casb18030026

Sodoudi, S., Zhang, H., Chi, X., Müller, F., Li, H., (2018), The influence of spatial configuration of green areas on microclimate and thermal comfort, Urban Forestry & Urban Greening, https://doi.org/10.1016/j.ufug.2018.06.002

Sola, A. Corchero, C., Salom, J., Sanmarti, M. (2020) 'Multi-domain urban-scale energy modelling tools: A review', Sustainable Cities and Society, 54. doi: 10.1016/j.scs.2019.101872

Speak, A., Montagnani, L., Wellstein, C., Zerbe, S. (2020). The influence of tree traits on urban ground surface shade cooling. Landscape and Urban Planning, 197. https://doi-org.proxy.library.lincoln.ac.uk/10.1016/j.landurbplan.2020.103748

Streiling, S., Matzarakis, A. (2003). Influence of single and small clusters of trees on the bioclimate of a city: A case study. Journal of Arboriculture, 29, 309-316

Talukdar, M., Hossen, M. and Baten, M. (2018). Trends of Outdoor Thermal Discomfort in Mymensingh: an Application of Thoms' Discomfort index. J. Environ. Sci. & Natural Resources, 10(2): 151-156.

Tanaka, K., Hashimoto, S.(2006). Plant canopy effects on soil thermal and hydrological properties and soil respiration. Ecological Modelling, 196(1-2),32-44. https://doi.org/10.1016/j.ecolmodel.2006.01.004

Thom, E.C. (1959).The discomfort index, Wetherwise, 12(2): 57-61. http://dx.doi.org/10.1080/00431672.1959.9926960

Upadhyay, G., Mauree, D., Kämpf, J., Scartezzini, J-L. (2015). Evapotranspiration model to evaluate the cooling potential in urban areas - A case study in Switzerland

Vieira de Abreu-Harbich, L., Labaki, L. C., Matzarakis A. (2015). Effect of tree planting design and tree species on human thermal comfort in the tropics. Landscape and Urban Planning, 138, 99-109 http://dx.doi.org/10.1016/j.landurbplan.2015.02.008

Walter E., Kämpf, J.H. (2015). A verification of CitySim results using the BESTEST and monitored consumption values. Proceedings of the 2nd Building Simulation Applications conference; 2015: Bozen-Bolzano University Press

Watts N, Amann M, Arnell N, Ayeb-Karlsson S, Belesova K, Berry H, Bouley T, Boykoff M, Byass P, Cai W, Campbell-Lendrum D, Chambers J, Daly M, Dasandi N, Davies M, Depoux A, Dominguez-Salas P, Drummond P, Ebi KL, Ekins P, Montoya LF, Fischer H, Georgeson L, Grace D, Graham H, Hamilton I, Hartinger S, Hess J, Kelman I, Kiesewetter G, Kjellstrom T, Kniveton D, Lemke B, Liang L, Lott M, Lowe R, Sewe MO, Martinez-Urtaza J, Maslin M, McAllister L, Mikhaylov SJ, Milner J, Moradi-Lakeh M, Morrissey K, Murray K, Nilsson M, Neville T, Oreszczyn T, Owfi F, Pearman O, Pencheon D, Pye S, Rabbaniha M, Robinson E, Rocklöv J, Saxer O, Schütte S, Semenza JC, Shumake-Guillemot J, Steinbach R, Tabatabaei M, Tomei J, Trinanes J, Wheeler N, Wilkinson P, Gong P, Montgomery H, Costello A. The 2018 report of the Lancet Countdown on health and climate change: shaping the health of nations for centuries to come. Lancet. 2018 Dec 8;392(10163):2479-2514. doi: 10.1016/S0140-6736(18)32594-7. Epub 2018 Nov 28. Erratum in: Lancet. 2020 Jun 6;395(10239):1762. PMID: 30503045.

Wu, C., Fang, Y., Lin, Y., Ma, X., Wang, Y., Wang, K. (2016). Analysis of the effect of street greenbelt on microclimate in a hot-humid area of China using a numerical simulation method, Journal of Meteorology and Environment, 32(5), 99-106. doi：10.3969/j.issn.1673-503X.2016.05.014

Wu, F., Zhu, C., Li, S.. (2013). Seasonal Changes of Temperature and Humidity of Six Urban Underlying in Beijing. Journal of Northwest Forestry University. 28(1)：207-213. DOI:10.3969/j.issn.1001-7461.2013.01.42

Wu, R., Yan, H., Shu, Y., Shi, Y., Bao, Z. (2019). Microclimatic Characteristics and Human Comfort Conditions of Bamboo Plant Communities in Summer, Chinese Landscape Architecture,35(7),112-117. doi: 10.19775/j.cla.2019.07.0112

Wu, S., Dong, L., Fan, S. (2020). Effect of land cover types on lowering air temperature and increasing humidity and human comfort level, 49(4),532-539. DOI:10.13323/j.cnki.j.fafu(nat.sci.).2020.04.016

Xue, F., Gou, Z., Lau, S. S. Y. L. (2017). Green open space in high-dense Asian cities: Site configurations, microclimates and users' perceptions. Sustainable Cities and Society, 34, 114-125. DOI: http://dx.doi.org/10.1016/j.scs.2017.06.014

Xue, X., Yang, J., Zheng, Y., Zhang, J., Zhuang, J., Cheng, J., Yang, D. (2016).Microclimate Characteristics of *Liriodendron chinense tulipifera* Forest in Nanjing. Research of Soil and Water Conservation, 04, 226-232. DOI: 10.13869/j.cnki.rswc.20160513.007

Yan, H., Wang, X., Hao, P., Li, D. (2012). Microclimatic characteristics and human comfort conditions of tree communities in northern China during summer. Journal of Beijing Forestry University, 34(5), 57-63. DOI: 10.13332/j.1000-1522.2012.05.021

Zölch, T., Rahman, M. A., Pfleiderer, E., Wagner, G., Pauleit, S. (2019). Designing public squares with green infrastructure to optimize human thermal comfort. Building and Environment, 149, 640-654. https://doi.org/10.1016/j.buildenv.2018.12.051

Zhao, Q., Sailor, D. J., Wentz, E. A. (2018). Impact of tree locations and arrangements on outdoor microclimates and human thermal comfort in an urban residential environment. Urban Forestry & Urban Greening, 32, 81-91. https://doi.org/10.1016/j.ufug.2018.03.022

Zheng, Y., Zhu, S., Fang, M., Wu, H., Yan, H., Shao, F. (2020). Relationships between Different Types of Plant Arrangement and Temperature-humidity Effects in Urban Parks. Journal of Northwest Forestry University, 35(3),243-249. doi: 10.3969/j.issn.1001-7461.2020.03.39

List of Tables

List of Figures

APPENDIX: Composition used in CitySim simulation

Composition of surrounding building floor in CitySim simulation

<Composite id="10" name="LesosaiBTK B 1" category="Floor">

<Layer Thickness="0.1000" Conductivity="2.3000" Cp="1000" Density="2300" NRE="0" GWP="0" UBP="0"/>

<Layer Thickness="0.0500" Conductivity="0.0300" Cp="1400" Density="50" NRE="0" GWP="0" UBP="0"/>

<Layer Thickness="0.0001" Conductivity="0.2000" Cp="1400" Density="960" NRE="0" GWP="0" UBP="0"/>

<Layer Thickness="0.0500" Conductivity="0.8500" Cp="1000" Density="1200" NRE="0" GWP="0" UBP="0"/>

<Layer Thickness="0.0100" Conductivity="1.3000" Cp="838.799988" Density="2300" NRE="0" GWP="0" UBP="0"/>

</Composite>

Composition of surrounding building roof in CitySim simulation

<Composite id="12" name="LesosaiBTK D 1" category="Roof">

<Layer Thickness="0.0500" Conductivity="1.4800" Cp="1100" Density="2400" NRE="0" GWP="0" UBP="0"/>

<Layer Thickness="0.0010" Conductivity="0.2000" Cp="1600" Density="1200" NRE="0" GWP="0" UBP="0"/>

<Layer Thickness="0.1600" Conductivity="0.0400" Cp="600" Density="120" NRE="0" GWP="0" UBP="0"/>

<Layer Thickness="0.0001" Conductivity="0.2000" Cp="1400" Density="960" NRE="0" GWP="0" UBP="0"/>

<Layer Thickness="0.2000" Conductivity="1.6000" Cp="1000" Density="2200" NRE="0" GWP="0" UBP="0"/>

Composition of surrounding building wall in CitySim simulation

<Composite id="57" name="Jill" category="Wall">

<Layer Thickness="0.0300" Conductivity="1.3000" Cp="838.799988" Density="2300" NRE="0" GWP="0" UBP="0"/>

<Layer Thickness="0.0600" Conductivity="2.3000" Cp="1000" Density="2300" NRE="0" GWP="0" UBP="0"/>

<Layer Thickness="0.0240" Conductivity="0.0360" Cp="601.200012" Density="60" NRE="0" GWP="0" UBP="0"/>

<Layer Thickness="0.0000" Conductivity="2.3000" Cp="1000" Density="2300" NRE="0" GWP="0" UBP="0"/>

</Composite>